THE EFFECT OF AUSTENITE VOLUME FRACTION ON THE DEFORMATION RESISTANCE OF 409 STAINLESS STEELS DURING HOT-STRIP ROLLING

D. Chae, S. Lee, S. Son

The mill log data obtained from the hot-strip rolling of 409 stainless steels were analyzed in order to investigate the effect of the chemical composition on the deformation resistance. The results showed that the deformation resistance depended sensitively on the austenite stabilizing capability of the material chemistry, suggesting the austenite volume fraction as a dominant factor in controlling the deformation resistance. Deformation resistance ratio (DRR) was defined as a ratio of the deformation resistance of a two-phase (ferritic+austenitic) microstructure to that of a fully ferritic microstructure. The dependence of DRR on the austenite volume fraction appeared to be linear, which was also observed by the plane strain compression tests performed on the laboratory specimens with various austenite volume fractions. The implication of this result is that during the hot-strip rolling of 409 stainless steels with a two-phase microstructure, these steels are likely to deform in an equal-strain manner.

KEYWORDS: 409 stainless steel, mean flow stress, deformation resistance, two-phase material, austenite potential and mill log analysis

INTRODUCTION

In hot-strip rolling, precise thickness control requires an accurate prediction of the roll force. The accurate prediction of the roll force, in turn, depends on the accurate calculation of the hot flow strength of the material because it significantly affects the pressure at the interface between the work roll and the rolled material. In order to calculate the hot flow strength as a function of rolling parameters which are representative of each rolling pass, an average flow strength, hereafter called 'deformation resistance' is defined over the total applied strain during a rolling pass[1, 2]. Industrially, deformation resistance is analyzed using mill log data to develop and refine rolling mill models.

The 409 stainless steels are characterized by relatively low carbon and nitrogen contents with approximately 11% chromium in their chemical compositions (Tab. 1). Titanium (and/or niobium) is usually added enough to tie up carbon and nitrogen atoms. Due to the fact that titanium is a strong ferrite former, these steels are fully ferritic in an annealed condition.

UNS	Composition percentage, max or range				
	C	N	Cr	Ni	Other elements
S40910	0.030	0.030	10.5-11.7	0.5	Ti 6(C+N) min, 0.5 max; Nb 0.17 max
S40920				0.5	Ti 8(C+N) min, Ti 0.15-0.5; Nb 0.10 max
S40930				0.5	Ti+Nb 0.08+8(C+N) min, 0.75max; Ti 0.05 min
S40945				0.5	Nb 0.18-0.40, Ti 0.05-0.20
S40975				0.5-1.0	Ti 6(C+N) min, 0.75 max

Tab. 1 **Chemical compositions of ferritic stainless steel grades containing 11% chromium in ASTM A 240/A 240M-00.**
Composizione chimica dei gradi di acciaio inossidabile ferritico contenenti 11% cromio negli ASTM A 240/A 240M-00.

Dongchul Chae, Soochan Lee, Seunglak Son
Posco, Pohang, Korea

Paper presented at the 3rd International Conference Thermomechanical Processing of Steels, organised by AIM, Padova, 10-12 September 2008

ID	C	Cr	Ni	Ti	Ni-equivalent	Cr-equivalent
A	0.007	9.5	0.1	0.2	0.57	12.64
B	~	~	~	~	0.80	12.65
C	0.010	11.5	2.0	0.3	0.93	12.43
D					1.02	11.98
F					2.46	10.86

Tab. 2
Chemical compositions of five plates (wt%). Ni-equivalent and Cr-equivalent are defined as Ni+0.5Mn+30C+0.3Cu+25N and Cr+2.0Si+1.5Mo+5.5Al+1.5Ti, respectively [10].
Composizione chinica di cinque lastre (wt%). Equivalenti di Ni e equivalenti di Cr sono definiti come Ni+0.5Mn+30C+0.3Cu+25N e Cr+2.0Si+1.5Mo+5.5Al+1.5Ti, rispettivamente [10].

However, it has been reported that these steels may contain austenite as a second phase at hot rolling temperatures [3]. Therefore, the present work aims at examining the influence of the presence of austenite on the deformation resistance of 409 stainless steels.
The industrial mill logs have been used to analyze deformation resistance as described elsewhere [4-7]. Most of the previous studies have used the mill log analysis on the carbon steels, where the strain accumulation and recrystallization between the rolling stands are important microstructural phenomena to be analyzed for controlling the microstructure. However, there has been no study on the effect of the presence of austenite on the deformation resistance of 409 stainless steels.
The prediction of the hot flow strength of the two-phase material is difficult because the partitioning of stress and strain is influenced by many factors [8]. The principal intrinsic and extrinsic factors which can affect the hot flow strength of the two-phase material are the phase morphology and the mode of deformation, respectively. The plane strain compression results on the wrought duplex stainless steels by Iza-Mendia et. al. [9] implies the equal-strain condition as an useful assumption, where the hot flow strength of the two-phase material is simply calculated from the strength of the each constitutive phase and its volume fraction [8-9]. In the current study, an attempt has also been made to check if the equal-strain criterion is a reasonable assumption in predicting the deformation resistance of 409 stainless steels, where the cumulative alloy contents are much smaller than the duplex stainless steels mentioned above. For this purpose, specimens were cast and hot-rolled in a laboratory to produce various austenite volume fractions and the plane strain compression tests were performed at a high temperature. Of particular interest is whether the equal strain condition is supported by the mill log analyses.

EXPERIMENTAL

The primary goal of the current study is to investigate the effect of austenite volume fraction on the flow strength in a plane strain compression mode of deformation. This can be accomplished by preparing the materials with the various austenite volume fractions. For this purpose, five materials were cast in a laboratory. Tab. 2 lists the chemical composition of the materials. The 50 kg ingots were initially hot-rolled into 20mm thick plates. These had been heat-treated at 1050 °C for 1 hour and subsequently hot-rolled into 12mm thick plates.
The plane strain compression specimens were machined from the 12mm thick plates such that the applied compression loading axis corresponded to the thickness direction of the plate. The plane strain specimen geometry used is shown in Fig. 1. The hot plane strain compression tests were performed at 1050°C and at a strain rate of 5/sec using a Gleeble 3800. The relatively large strain (equivalent strain of 0.7) response of the material was determined. After unloading the plane strain compression specimen, the width expansion was measured with a measuring microscope and approximately 12% width expansion was observed.
Log data were collected from the POSCO's seven-stand hot strip mill, Pohang, Korea. In order to calculate true strains, strain rates, and deformation resistances, the following log data were used; strip width, strip entry and exit thicknesses, work roll diameter, work roll rotational speed, roll force, and strip entry temperature predicted according to a model for each pass. In addition, the Sims's equation was employed to calculate deformation resistances and the roll flattening was also taken into account [4-7].

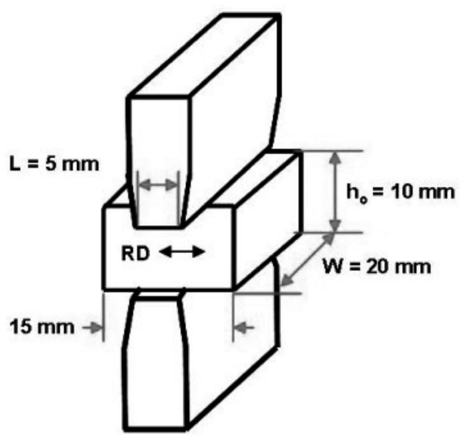

Fig. 1
Specimen geometry of plane strain compression testing.
Geometria dei campioni della prova di deformazione da compressione del piano.

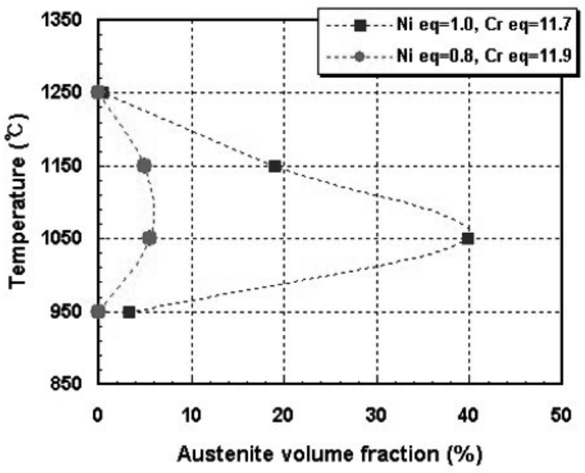

Fig. 2

The effect of chemical composition on the austenite volume fraction. The two ingots were quenched after the heat treatment at 950~1250°C for 1 hour.

Effetto della composizione chimica sulla frazione in volume del austenite. I due lingotti sono stati temprati dopo trattamento termico a 950~1250°C per 1 ora.

DISCUSSION

The Shaffler diagram represents the as-solidified microstructure after a rapid cooling as a function of Cr-equivalent and Ni-equivalent [10]. It is noteworthy that the compositional range of 409 stainless steels is near the two-phase (martensitic+ferritic) boundary in the Shaffler diagram.

Because the presence of martensite implies the thermal transformation from austenite, it is likely that the material may have an austenite phase at high temperatures. This seems to be closely related to one of the significant features of the Fe-Cr equilibrium diagram, that is, the phase boundary between austenite and ferrite fields, known as the gamma loop. Based on the Fe-Cr equilibrium diagram, approximately 11% Cr is near the nose of the gamma loop. Therefore, austenite is likely to form at high temperatures. In addition, it is also well known that the role of austenite stabilizing elements such as carbon and nitrogen is to shift the gamma loop to higher chromium content. Therefore, the small fluctuation in the austenite stabilizing capability of the material chemistry can possibly affect the phase balance between ferrite and austenite significantly.

It can be seen in Fig. 2 that, for two 409 ingots produced in a laboratory, the high temperature microstructure consists of two phases, austenite+ferrite, and the maximum amount of austenite occurs at about 1050 °C.

The microstructures of the 12mm thick hot rolled plates exposed at 1050°C for 5 minutes are shown in Fig. 3. The microstructure of the material A (in Tab. 2) is observed to be fully ferritic as shown in Fig. 3(a). The region of light contrast in Fig. 3(b) corresponds to the elongated martensite transformed from austenite. As the Ni-equivalent of the materials increases, the banded array of alternating layers of ferrite and martensite (i.e., austenite) becomes distinctive. The consequence of the highest Ni-equivalent is the formation of a 100% martensitic microstructure (Fig. 3(e)).

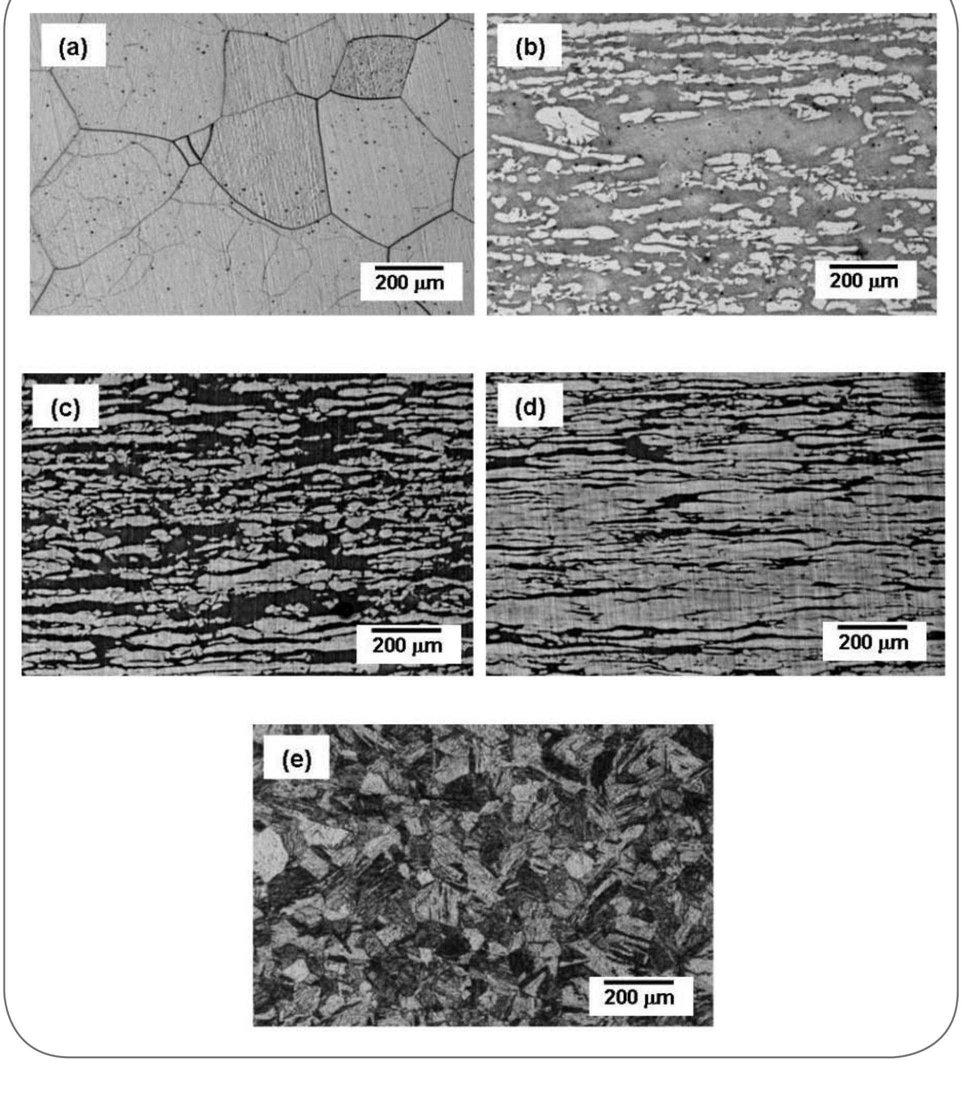

Fig. 3

Light micrographs quenched after the heat treatment at 1050°C for 5 minutes in the case of (a) the material A, (b) the material B, (c) the material C, (d) the material D and (e) the material F in Table 2. Murakami etchant was used for etching.

Micrografie di pezzi temprati dopo trattamento termico a 1050°C per 5 minuti nel caso del (a) materiale A, (b) materiale B, (c) materiale C, (d) materiale D e (e) materiale F di Tebella 2. Per l'attacco chimico è stato utilizzato il reagente di Murakami.

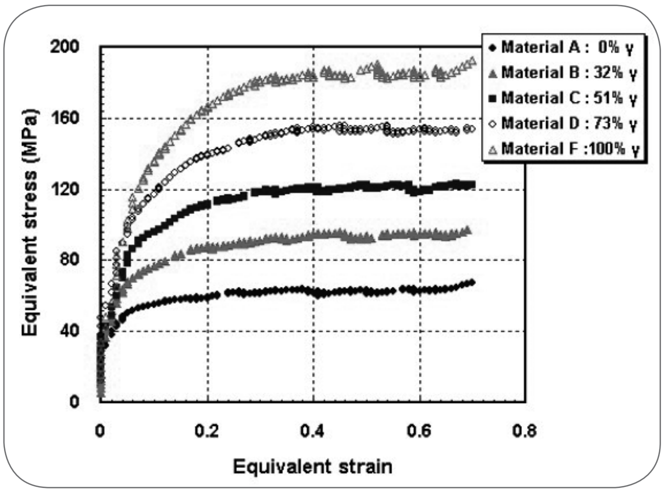

Fig. 4

Compressive stress-strain responses of the materials with the chemical compositions and the microstructures shown in Table 2 and Fig. 3, respectively.

Risposta sforzo a compressione-deformazione dei materiali con composizione chimica e microstruttura mostrati rispettivamente in Tab 2 e Fig 3.

The plane strain compression tests were performed on the specimens machined from the materials in Tab. 2 at a strain rate of 5/s and at 1050°C. Austenite volume fractions were also measured using an image analysis technique on the specimens quenched before compression. The measured values were, 0, 32, 51, 73, and 100% as shown in Fig. 4. As the amount of the austenite increases, the higher degree of strain-hardening is observed on a flow curve. The distinctively different strain hardening behaviours results in the significantly different flow stress levels at large strains.
Thus, these results indicate that the austenite volume fraction plays a major role in increasing the flow stress.
In order to quantify the effect of austenite volume fraction on the hot flow strength, the mean flow stress at a certain strain is defined from the stress-strain curve obtained from the plane strain compression tests.

$$MFS = \frac{1}{\varepsilon_{eq}} \cdot \int_0^{\varepsilon_{eq}} \sigma \cdot d\varepsilon_{eq} \quad [1]$$

The mean flow stresses at an equivalent strain of 0.5 were shown in Fig. 5(a) as a function of austenite volume fraction. The sensitivity of the MFS to the austenite volume fraction appears to be linear. This linear relationship may be explained by Equ. 2.

$$\begin{aligned} MFS_{\alpha+\gamma} &= MFS_\alpha \cdot f_\alpha + MFS_\gamma \cdot f_\gamma \\ &= MFS_\alpha + (MFS_\gamma - MFS_\alpha) \cdot f_\gamma \end{aligned} \quad [2]$$

where, $f\alpha$ and $f\gamma$ are the volume fraction of ferrite and the volume fraction of austenite, respectively.

Deformation resistance ratio (DRR) is defined as a ratio of the MFS of a two-phase (ferrite+austenite) microstructure to that of a fully ferritic microstructure by adopting so called "the mixture rule" as indicated in Equ. 2.

$$DRR = \frac{MFS_{\alpha+\gamma}}{MFS_\alpha} = 1 + \left(\frac{MFS_\gamma}{MFS_\alpha} - 1 \right) \cdot f_\gamma \quad [3]$$

The dependence of DRR on austenite volume fraction is shown in Fig. 5(b). The deformation of coarse two-phase microstructures depends on whether the material obeys an equal-stress condition (in which strain can concentrate in one of the microconstituents) or if an equal-strain condition applies to the constituents. Given the elongated morphology of the microstructure as shown in Fig. 3, we expect that the equal-strain condition to be obeyed for deformation with the plane strain compression axes along the thickness direction. The linear dependence of DRR on austenite volume fraction as shown in Fig. 5(b) implies that the equal-strain condition is closely followed.
The deformation resistance was calculated using the fol-

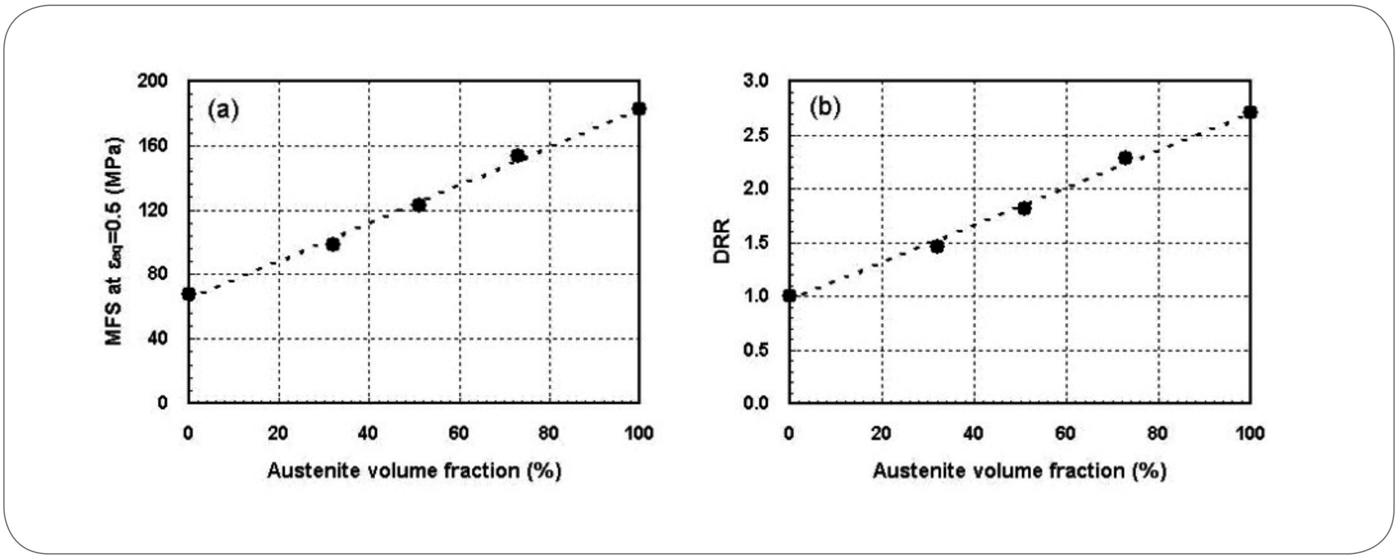

Fig. 5

Dependences of (a) mean flow stress and (b) DRR on austenite volume fraction.

Dependenza di (a) sollecitazione di flusso media e (b) DRR su frazione di volume di austenite.

Material	Chemical composition (wt%)					Austenite volume fraction before F1 (%)
	C	N	C+N	Cr-equivalent	Ni-equivalent	
M1	0.005	0.005	0.010	12.95	0.68	~0
M2	~	~	~	12.48	0.75	7
M3	0.015	0.010	0.025	12.20	0.93	33
M4				13.03	0.48	~0

Tab. 3

Chemical compositions of the four materials(wt%) and their austenite volume fraction observed before the entry to the first pass, F1, of the hot–strip finishing mill. Ni-equivalent and Cr-equivalent are defined as Ni+0.5Mn+30C+0.3Cu+25N and Cr+2.0Si+1.5Mo+5.5Al+1.5Ti, respectively.

Composizione chimica dei quattro materiali (% in peso) e loro frazione di austenite (in volume) rilevata dopo ingresso alla prima passata, F1, nel laminatoio di finitura. Ni e Cr equivalenti definiti rispettivamente come Ni+0.5Mn+30C+0.3Cu+25N e Cr+2.0Si+1.5Mo+5.5Al+1.5Ti.

lowing equation:

$$K_m = \frac{P}{B \cdot L_d \cdot Q_p}$$

where, P, B, Ld and Qp are roll force, strip width, the projected length of the arc of contact between the roll and the rolled material and Sims geometrical factor, respectively. It should be reminded that the MFS obtained from the stress-strain curve can be compared to the deformation resistance obtained from the rolling data. Thus, MFS in Equ. 2 were replaced with Km. Then, the DRR is also defined from the deformation resistance calculated from the mill log data.

$$DRR = \frac{K_{m,\alpha+\gamma}}{K_{m,\alpha}} = 1 + \left(\frac{K_{m,\gamma}}{K_{m,\alpha}} - 1\right) \cdot f_\gamma \quad [5]$$

where, $K_{m,\alpha}$ and $K_{m,\gamma}$ are the deformation resistances of a single ferritic microstructure and a single austenitic microstructure, respectively.

The dependence of deformation resistance on the entry temperature was analyzed from the first rolling pass, F1, to the last rolling pass, F7. Four materials were examined in details. The differences in the composition and the microstructure are summarized in Tab. 3. Among the four materials, it was observed that M2 and M4 had two phase (ferrite+austenite) microstructures right before the entry to F1. The austenite volume fractions of M2 and M3 materials right before the entry to F1 were measured to be 7% and 33% as shown in Fig. 6, respectively while austenite formation was not found from the M1 and M4 materials.

The rolling conditions for the materials, M2, M3 and M4, were also much similar to those of M1 except for the entry temperatures. It is a usual occurrence that if the rolling temperature increases, then the deformation resistance decreases. This usual expectation is confirmed from the observation that the deformation resistance of the fully ferritic M4 is lower at the same pass than that of the fully ferritic M1 because the rolling temperature of M4 was higher than that of M1. However, comparing the responses of M1 with those of M2 and M3, a significant trend is observed (Fig. 7(a)). The deformation resistances of the two-phase materials, M2 and M3 are higher than that of the fully ferritic material, M1, even though the rolling temperatures were higher in the case of M2 and M3.

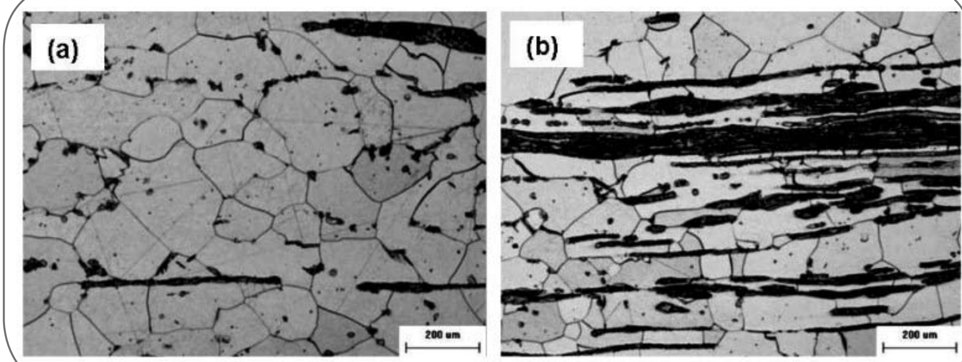

Fig. 6

Microstructures of (a) the material M2 and (b) M3. Martensitic phases (i.e., high temperature austenitic phases) with dark contrast are elongated along the rolling direction.

Microstrutture di (a) il materiale M2 e (b) materiale M3. Con contrasto scuro le fasi martensitiche (ex fasi austenitiche alle alte temperature) con contrasto scuro sono allungate lungo la direzione di laminazione.

This unexpected behaviour can be understood by the presence of the higher volume fraction of hard austenite in the microstructure of the materials, M2 and M3.

An attempt was made to calculate the DRR values during the first pass, F1, for the materials shown in Tab. 3. In order to calculate the DRR, the dependence of deformation resistance on the entry temperature must be known for the fully ferritic material. Therefore, additional mill logs were analysed. Twenty seven materials with six different chemical compositions were selected for the investigation. The applied strains were in the range of 0.45~0.50 and the strain rates were between 7.5 to 9.5/sec. Thus, the rolling conditions except for the temperature were almost constant. The samples for the microstructural examination were taken right before the entry to the first pass, F1, and all the microstructures investigated using an optical microscope were

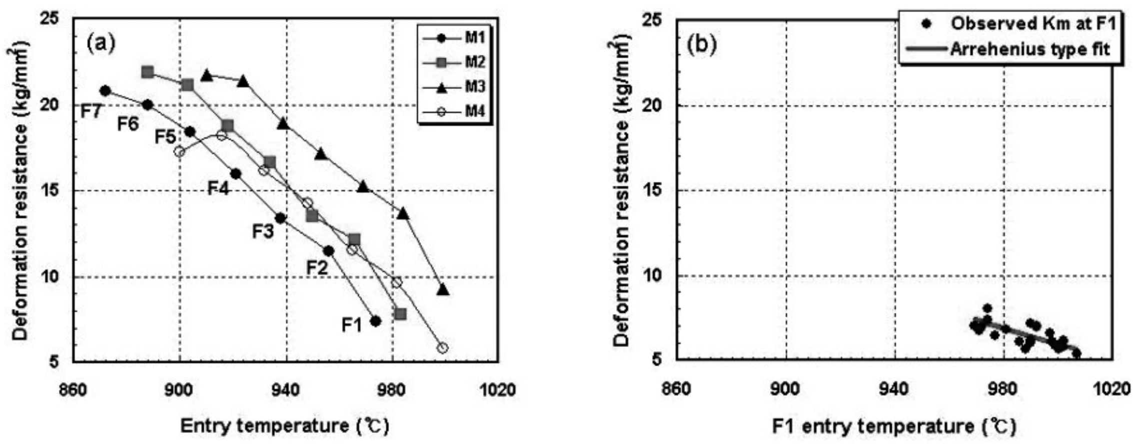

Fig. 7
The deformation resistances of (a) the materials (Table 3) during rolling passes and (b) the materials with a single ferritic microstructure during the first rolling pass, F1.
Resistenza alla deformazione dei (a) materiali (Tab. 3) durante i passaggi di laminazione e (b) i materiali con una singola microstruttura ferritica durante il primo passaggio di laminazione, F1.

found to be ferritic. The calculated values of the deformation resistances during the first pass, F1, were analyzed together and Arrehenius type of temperature dependence of deformation resistance was obtained as follows:

$$K_{m,\alpha} = A \cdot \exp\left(\frac{B}{T(K)}\right) \qquad [6]$$

where, A and B are constants [12]. The values of the constants, A and B, are $7.9x10^{-4}$kg/mm2 and $11.36x10^{3}$K, respectively. The Arrehenius type fit was compared with the calculated deformation resistance data during the first pass, F1 (Fig. 7(b)).
The DRR was evaluated by inserting Equ. (6) into Equ. (5). The calculated DRR as a function of austenite volume fraction was shown in Fig. 8(a) for the materials, M1, M2, M3 and M4. These data imply that the DRR values calculated from the mill log analysis are quite close to those obtained from the plane strain compression results as shown in Fig. 8(a). This is understandable because the strains and the strain rates considered were quite similar between the mill log analyses during the first rolling pass, F1, and the plane strain compression tests performed in this study. The influence of solute content on the ability to form austenite at hot rolling temperature was predicted in terms of the austenite potential based on thermodynamic calculations using a commercial software package, ThermoCalc. Austenite potential (%) is defined as austenite mass fraction at 1000°C. As shown in Fig. 8(b), The DRR increases as the austenite potential increases.
Therefore, it implies again that the DRR values depend sensitively on the austenite stabilizing capability of the material chemistry.
Finally, the DRR values during the first pass, F1, calculated from the twenty eight materials with different chemical compositions were shown as a function of austenite potential (Fig. 9(a)). The rolling conditions such as the strains and the strain rates were also very similar. It is interesting to note that the DRR values approximately become one if the austenite potential is equal to or lower than about 50%. At these low levels of the austenite potential, the optical microstructures examined from the samples taken right before the entry to F1 were fully ferritic. The effect of the chemical composition on DRR was shown in Fig. 9(b). It is clearly seen that the DRR increases as Ni-equivalent increases and Cr-equivalent decreases. The implication of Fig. 9(b) is that small fluctuations in Ni-equivalent and Cr-equivalent can significantly change the phase balance between ferrite and austenite at hot-strip rolling temperatures.

CONCLUSION

The deformation resistances of 409 stainless steels during hot-strip rolling were investigated to understand the influence of the presence of austenite at high temperatures on the rolling force.
Although the commercially cold-rolled and annealed sheet products of 409 stainless steels are essentially ferritic in an as-annealed state, these steels can have a two-phase microstructure (ferrite+austenite) during hot-strip rolling, which depends on the chemical composition. The hot plane strain compression tests were performed on the specimens, cast and hot-rolled in a laboratory, with different austenite volume fractions. The tests clearly showed the significant role played by the austenite volume fraction in controlling the strain hardening behaviour of the two-phase microstructure. As a result, the mean flow stress at an equivalent strain of 0.5 was found to be approximately a linear function of the austenite volume fraction. The mill data from the hot-strip rolling were analyzed in order to calculate the deformation resistance developed in the roll gap of the rolling stand. Based on the Sims's model, the calculated deformation resistances were found to depend sensitively on the austenite stabilizing capability of the material chemistry. Accordingly, the influence of the solute content on the ability to form austenite at hot rolling temperatures was predicted in terms of the austenite potential which is defined as the austenite mass fraction at 1000°C. The deformation

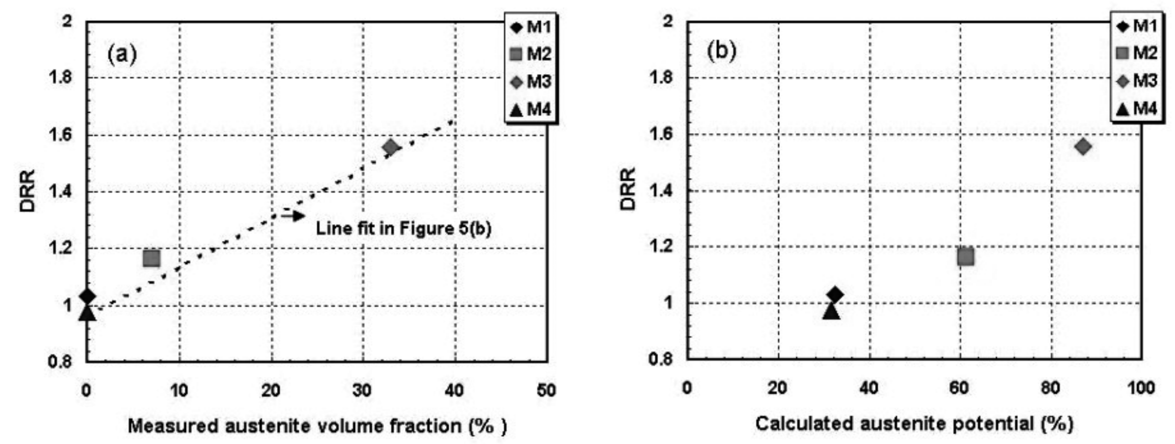

Fig. 8

The dependence of DRR as a function of (a) the measured austenite volume fraction and (b) the calculated austenite potential. The line fit in Fig. 5(b) was superimposed to compare the DRRs from the experiments with those from the mill log analyses.

Variazione del DRR in funzione di (a) frazione in volume dell'austenite misurata e (b) potenziale di austenite calcolato. La linea inserita in Fig. 5(b) è stata aggiunta per confrontare i DRR delle sperimentali con quelli dedotti dall' analisi dei documenti di produzione.

resistance ratio (DRR) was defined as a ratio of the deformation resistance of a two-phase microstructure to that of a fully ferritic microstructure. The DRR appears to vary linearly with the austenite volume fraction, thus implying that the material is likely to deform in an equal-strain manner along the hot rolling direction.

REFERENCES

1) William L. Roberts, Hot Rolling of Steels, Marcel Dekker Inc., 1983, p.649

2) Vladimir B. Ginzburg and Robert Ballas, Flat Rolling Fundamentals, Marcel Dekker Inc., 2000, p.199

3) Robert G. Nooning, Jr., Master Thesis, University of Pittsburgh, 2002, p76.

4) T. M. Maccagno, J. J. Jonas, S. Yue, B. J. McCrady, R. Slobodian and D. Deeks, ISIJ International, Vol. 34, 1994, No. 11, p.917.

5) T. M. Maccagno, J. J. Jonas and P. D. Hodgson, ISIJ International, Vol. 36, 1996, No. 6, p.720.

6) F. Siciliano Jr., K. Minami, T. M. Maccagno and J. J. Jonas, ISIJ International, Vol. 36, 1996, No. 12, p.1500.

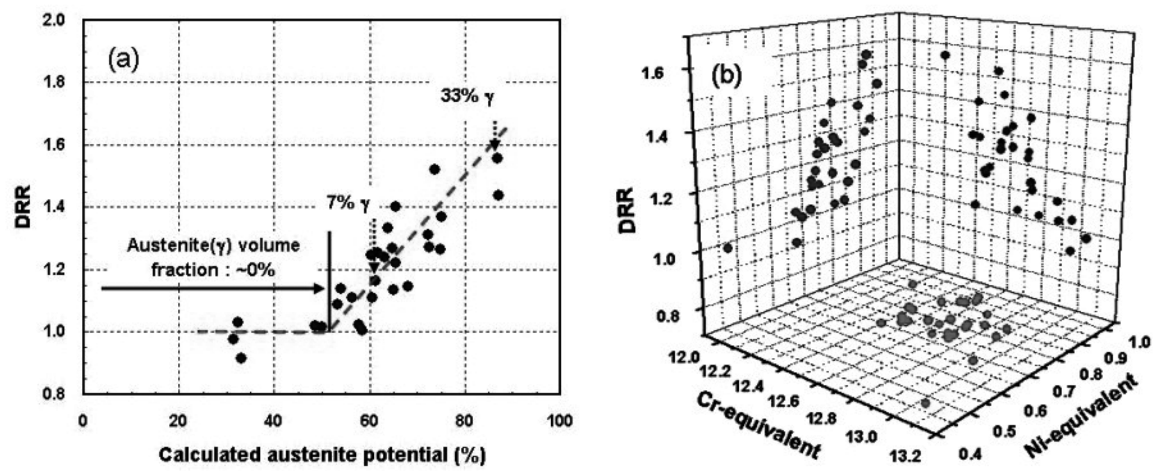

Fig. 9

The dependence of DRR during a first rolling pass, F1, as a function of (a) the calculated austenite potential and (b) the Cr-equivalent & Ni-equivalent. Three dimensional data have been projected on the two dimensional planes in Fig. 8(b).

La dipendenza del DRR durante il primo passaggio di laminazione, F1, in funzione di (a) potenziale di austenite calcolato e (b) Cr e Ni equivalenti. I dati tridimensionali sono stati proiettati sui piani bidimensionali di Fig. 8(b).

7) Fulvio Siciliano, Jr. and John J. Jonas, Metallurgical and Materials Transactions A, Vol. 31A, February (2000), p.511
8) Lode Duprez, Doctoral Thesis, Universiteit Gent, March (2003), p.97
9) A. Iza-Mendia, A. Pinol-Juez, J. J. Urcola, and I. Gutiérrez, Metallurgical and Materials Transactions A, Vol. 29A, February (1998), p.2975
10) George Krauss, Steels, ASM International, 2005, p.495
11) Shigeru Shida, Journal of the Japan Society for Technology of Plasticity, Vol. 9, No. 85, 1968-2, p.127

ABSTRACT

L'EFFETTO DELLA FRAZIONE IN VOLUME DELL'AUSTENITE SULLA RESISTENZA ALLA DEFORMAZIONE DEGLI ACCIAI INOSSIDABILI 409 DURANTE LA LAMINAZIONE A CALDO DI NASTRI

Parole chiave: acciaio inossidabile, laminazione a caldo

Nel presente lavoro sono stati analizzati i dati raccolti dal laminatoio per la produzione a caldo di nastri in acciaio inossidabile 409 al fine di esaminare l'effetto della composizione chimica sulla resistenza alla deformazione. I risultati hanno dimostrato che la resistenza alla deformazione dipende sensibilmente dalla possibilità di stabilizzare l'austenite tramite la composizione del materiale, suggerendo quindi che la frazione in volume di austenite sia il fattore dominante nel controllo della resistenza alla deformazione. Il rapporto di resistenza alla deformazione (DRR), è stato definito come un rapporto tra la resistenza alla deformazione di una microstruttura bifasica (ferritica + austenitica) rispetto a quella di una microstruttura pienamente ferritica. La dipendenza del DRR dalla frazione in volume di austenite si è dimostrata lineare, come è risultato anche dalle prove di deformazione da compressione del piano effettuate su campioni di laboratorio con diverse frazioni in volume di austenite. L'implicazione di questo risultato è che, durante la laminazione a caldo di nastri di acciaio inossidabile 409 con microstruttura a bifasica, questi acciai risultano predisposti alla deformazione in modo uniforme nella direzione di laminazione.